High Efficiency Dual-Bridge LLC Resonant Converter with Adaptive Frequency Control for On-Board Charger Applications

Tuyen D. Nguyen[1,2], Trinh Nguyen[1,2], Ravi Nath Tripathi[3], Long H. B. Nguyen[4], Minh V. Vo[4] and Hai N. Tran[4]
[1]Faculty of Electrical and Electronics Engineering, Ho Chi Minh City University of Technology (HCMUT), Ho Chi Minh City, Vietnam
[2]Vietnam National University Ho Chi Minh City, Linh Trung Ward, Thu Duc District, Ho Chi Minh City, Vietnam
[3] Nagamori Actuator Research Center, Kyoto University of Advanced Science, Kyoto, Japan
[4] XEVTECH Co., Ltd., Ba Ria - Vung Tau, Vietnam

***Abstract*-- This paper proposes an adaptive frequency control strategy for the unidirectional DC/DC converter based on Dual-bridge LLC (DBLLC) resonant converter to eliminate the circulating interval (CI), which causes high conduction loss. The LLC resonant converters are the preferred choice to select of DC/DC converter topology for on-board charger (OBC) due to it provides many advantages such as high efficiency, high power density. The DBLLC resonant converter operating with variable frequency and the pulse width-modulated (PWM) control will be applied as an isolated stage (DC/DC converter) of 400V-7.4 kW to improve the power density and efficiency of the whole system. The advantage of operating at the adaptive frequency is that the conduction loss in all devices will be reduced, while the soft switching technique is still achieved over the full load range. Furthermore, the detailed CI characteristic along with losses analysis is presented. The topology is designed for 400 VDC input to 220-380VDC output conversion, in the power range from 3.3 kW to 7.4kW. All theoretical analysis and the experimental results on the proposed converter are provided to verify the system performance.**

***Index Terms*-- DBLLC, Circulating period, Adaptive frequency, Onboard Charger.**

I. Introduction

Nowadays, the electric vehicle industry is developed dramatically. A hundred models of electric vehicles (EVs) from different brands were released for commercial purposes. Global EV sales reached 6.75 million units in 2021. Meanwhile, China is the largest market with 3.396 million units [1]. Since the battery electric vehicles (BEVs) are powered solely by an electric battery, with no fossil fuel engine parts thus they have zero carbon emissions and are friendly to the environment. Thus, consumer spending on EVs continues to rise, while the government supports stabilities. The structure of the BEVs is shown in Fig. 1. There are two chargers in the BEVs, the fast charger powered by the three-phase electric power has a high power-rating, and it has a fast-charging time (usually less than one hour), the OBC powered by the one-phase electric power has a low power rating, so the charging time is longer than the fast charger. Both chargers charge for the High Voltage (HV) battery which powers the inverter and

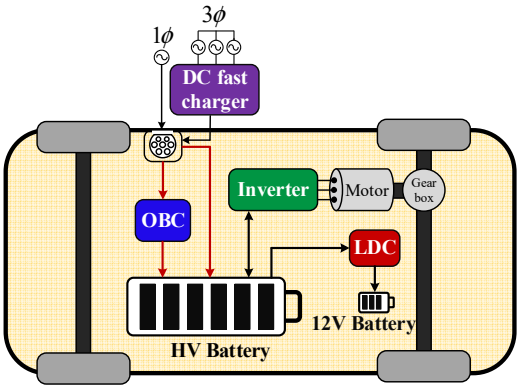

Fig. 1. The structure of the BEVs

the Low-voltage DC/DC Charger (LDC). The inverter plays a role as DC/AC converter to power the motor. The LDC charges the 12V battery powering electric devices in the car. For the traditional OBC, it consists of the power factor correction (PFC) and the DC-DC part. The OBCs are categorized as level-1 (<3.7kW), level-2 (3.7-22kW), and level-3 (22-43.5kW) chargers based on their power levels according to the SAE J1772 standard [2]. Currently, nearly every OBCs has a power rating at level 2 (6.6kW, 7.4kW, and 11kW). The trends of the EV industry are increasing the power level, improving power density, and improving the efficiency of the chargers including both fast chargers and on-board chargers. The OBC in this research follows the AC-Level 2 with the maximum power is 7.4kW, the power supply is single phase 240VAC electric power, the DBLLC converter plays an isolated and regulated voltage function in the OBC.

One of the most popular DC/DC converters is the LLC resonant converter, and it has been widely used in many different applications including OBC systems, distributed power systems, renewable energy generation systems, laptop adaptors, ... The structure of the conventional OBC using the Full-Bridge LLC converter is presented in [3]. The most frequently adopted modulation strategy for FB

LLC is the fixed switching frequency modulation strategy because, with this strategy, the soft-switching technique is achieved for both zero voltage switching (ZVS) turn-on and zero current switching (ZCS) turn-off. Therefore, it can reach high efficiency. With this strategy, the traditional FB LLC operates with characteristics like a DC transformer (DCX) [4], and the sophisticated design of the LLC resonant tank parameters as a DCX is also simplified since we do not need to consider the load characteristics. However, it can not regulate the output voltage to follow the charging profiles [5] of the battery, so if the FB LLC with this strategy control is applied in OBC systems, it plays only one function as an isolated stage.

The smart battery charger with two stages is proposed in [5], [6] with the DC/DC stage is the FBLLC resonant converter. For regulating an appropriate voltage that follows the charging profile of the Lithium battery, the pulse frequency modulation (PFM) strategy and the phase shift modulation (PSM) strategy are proposed. However, the PFM controller required a wide operating frequency to meet the DC gain requirement, and the wide switching frequency cause some problems [7]: complicated magnetic components and gate driver design, soft switching may not achieve for a full range of operation frequency, and poor electromagnetic interference (EMI) performance. The PSM can regulate the wide output voltage, but it is difficult to achieve the ZVS for all switches, and it needs to carefully design the value of inductance and capacitance in the resonant tank to reach the requirement specifications.

The DBLLC converter which is proposed in [6]-[7] is controlled by PWM strategy at fixed switching frequency. As also mentioned in previous research, the circulating period exists two times in each switching circle and during this time, there is no power transfer to the secondary side of the transformer. Therefore, the longer this time the larger conduction loss that all devices must be suffered. This may consequently have a significant effect on the performance of the converter. This paper proposes an adaptive frequency control for the DBLLC converter to eliminate the circulating interval and then applying the DBLLC converter into the OBC system because of some advantages. Firstly, this converter has the buck voltage function by controlling the duty of switches, so the output voltage can be controlled following the charging profile of the Lithium battery. Secondly, the soft switching (ZVS) is achieved for all switches, then the efficiency of the whole system will be improved. Furthermore, this paper presents the detailed transformer design procedure for the DBLLC converter to achieve the ZVS turn on for all main switches over a full range of battery voltage. The loss analysis is also presented to choose the appropriate switching frequency, select the devices, and calculate the efficiency of the converter.

II. OPERATION PRINCIPLES ANALYSIS

A. Topology Description and Operation Modes

The Dual-Bridge LLC converter is shown in Fig. 2. The DBLLC converter is implemented by adding a pair of anti-series Mosfet (S_{p5}-S_{p6}) between the midpoint of the switch leg (S_{p3}-S_{p4}) and the input capacitor leg (C_{in1} and C_{in2}).

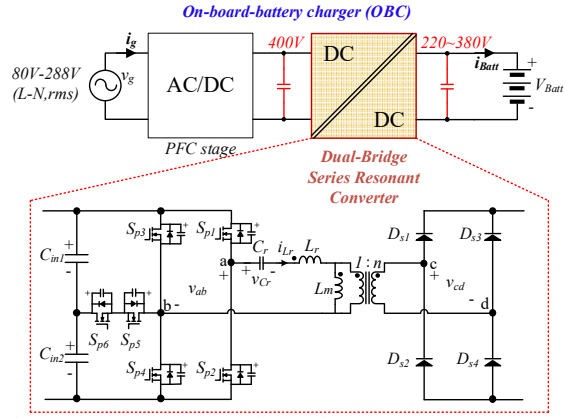

Fig. 2. Structure of OBC employing the DBLLC.

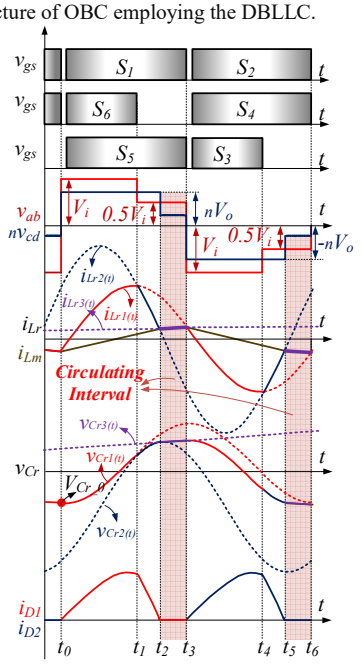

Fig. 3. Key operating waveforms of the DBLLC converter

Thus, the following two modes can be achieved by controlling the anti-series Mosfet S_{p5} and S_{p6}.

1) Half-Bridge LLC mode: When the anti-series Mosfets S_{p5}-S_{p6} are turned ON, the regulated output voltage is $\pm V_{in}/2$
2) Full-Bridge LLC mode: when S_{p5} or S_{p6} is turned off, the regulated voltage is $\pm V_{in}$

In this section, the operating principle of DBLLC converter operating at fixed-frequency equal to the series resonant frequency of resonant capacitor C_r and the resonant inductor L_r, $f_r = 1/2\pi\sqrt{L_r C_r}$ is presented. The gate signal of S_{p1} is complementary to the gate signal of S_{p2} with fixed-duty 0.5. The gate signal of S_{p3} is complementary with the gate signal of S_{p5}. Similar, the gate signal of S_{p4} is complementary with the gate signal of S_{p6}, but the gate signal of S_{p4} is shifted by a phase of π with that of S_{p3}. The duty of S_{p3} and S_{p4} is D which is the output of the controller. With this modulation scheme, the voltage stress of the switches S_{p5}, S_{p6} is always equal to V_{in} and haft, the voltage stress of the switches S_{p1}, S_{p2} is

always equal to V_{in}, and the voltage stress of the switches S_{p3}, S_{p4} has two levels: V_{in} or $V_{in}/2$.

B. Operation principles of the DBLLC controlled with the switching frequency equal to the resonant frequency.

The operation principle for the detailed interval including the process of charging, discharging on the junction capacitors to achieve the ZVS turn on, and also the process of body diodes conducting in the deadtime interval are analyzed in [6]-[7]. Therefore, this paper will focus on the three main intervals when the characteristics of resonant current and resonant voltage are different. The modulation strategy and the key operating waveforms are illustrated in Fig. 3. The results of the analysis are the equation of i_{Lr} and v_{Cr}, which help to define the specifications for the design process.

Interval 1[$t \in (0;t_1)$, Figs. 3, 4a and 5a]: In this interval, S_{p1}, S_{p4}, and S_{p5} turn on, the anti-series Mosfets leg do not conduct the current, so the v_{ab} equals Vin and the V_{cd} equals V_{Batt}. The source voltage across the resonant tank is V_{in}-nV_{Batt}. Thus, we can write:

$$v_{Lr} = V_{in} - nV_{Batt} - V_{Cr0} = L_r.\frac{di_{Lr}}{dt} \quad (1)$$

$$i_{Lr} = i_{Cr} = C_r.\frac{dv_{Cr}}{dt} \quad (2)$$

where v_{Cr} and i_{Lr} are the resonant capacitor voltage and resonant inductor current respectively. Combining (1) and (2) by using the Laplace method, i_{Lr} and v_{Cr} can be expressed as

$$i_{Lr1}(t) = \sqrt{\frac{C_r}{L_r}}.\left(V_{in} - nV_{Batt} - V_{Cr0}\right).\sin(\omega t) + i_{Lr}(0).\cos(\omega t) \quad (3)$$

$$v_{Cr1}(t) = (V_{in} - nV_{Batt}) - (V_{in} - nV_{Batt} - V_{Cr0}).\cos(\omega t) + \sqrt{\frac{L_r}{C_r}}.i_{Lr}(0).\sin(\omega t) \quad (4)$$

where V_{Cr0} and I_{Lr0} are the initial conditions at $t=0$,$\omega = 1/\sqrt{L_r C_r}$ is the resonant angular frequency.

Interval 2[$t \in (t_1; t_2)$, Figs.3, 4b and 5b]: In this time, the S_{p5}, S_{p6} leg is conducting. At interval 2, as shown in the equivalent circuit in Fig.5b, the only difference from interval 1 is that the V_{ab} equals $V_{in}/2$, the source voltage across the resonant tank is $0.5V_{in}$-nVB_{att}. Thus, we can write:

$$v_{Lr} = 0.5V_{in} - nV_{Batt} - v_{Cr1}(t_1) = L_r.\frac{di_{Lr}}{dt} \quad (5)$$

$$i_{Lr} = i_{Cr} = C_r.\frac{dv_{Cr}}{dt} \quad (6)$$

From (5) and (6), i_{Lr} and v_{Cr} in interval 2 are given by

$$i_{Lr2}(t) = \sqrt{\frac{C_r}{L_r}}.\left(0.5V_{in} - nV_{Batt} - v_{Cr1}(t_1)\right).\sin\omega(t-t_1) + i_{Lr1}(t_1).\cos\omega(t-t_1) \quad (7)$$

$$v_{Cr2}(t) = \left(0.5V_{in} - nV_{Batt}\right) + \sqrt{\frac{L_r}{C_r}}.i_{Lr1}(t_1).\sin\omega(t-t_1) - \left(0.5V_{in} - nV_{Batt} - v_{Cr1}(t_1)\right).\cos\omega(t-t_1) \quad (8)$$

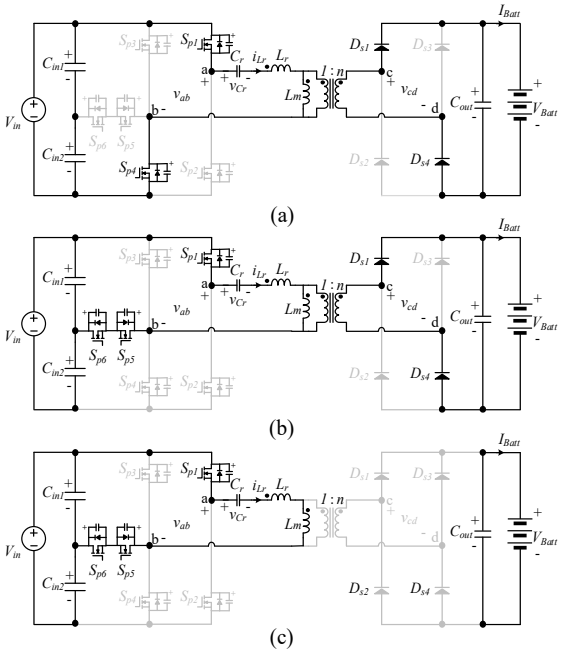

Fig. 4. Operating modes of DBLLC converter with f_s=f_r. (a) Interval 1 [t_0, t_1]. (b) Interval 2 [t_1, t_2]. (c) Interval 3 [t_2, t_3].

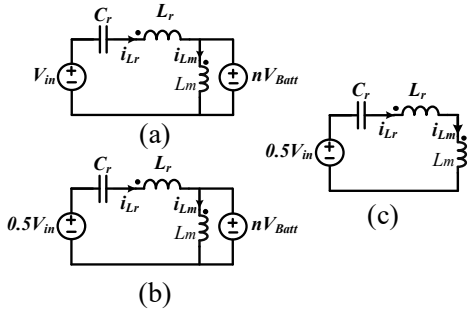

Fig. 5. Equivalent circuit of operating modes of DBLLC converter. (a) Interval 1 [0, t_1]. (b) Interval 2 [t_1, t_2]. (c) Interval 3 [t_2, t_3].

where $t_1=D.T_s$, D is a duty of the switches S_{p1} and S_{p4}.

Interval 3 [$t \in (t_2-t_3)$, Fig.3, 4c and 5c]: in this time, there is no difference of the gate signal of switches, but the resonant current equals to the magnetizing current in the inductor Lm, thus there is no current flowing through the secondary side. The output capacitor is discharged to power the battery. In this time, the magnetizing inductor L_m joins to resonate with L_r and C_r. The equivalent circuit is shown in Fig.5c, where C_r, L_r, and L_m form the series resonant tank.

$$v_{Lr} = 0.5V_{in} - v_{Cr}(t_2) = \left(L_r + L_m\right).\frac{di_{Lr}}{dt} \quad (9)$$

$$i_{Lr} = i_{Cr} = C_r.\frac{dv_{Cr}}{dt} \quad (20)$$

From (9) and (10), i_{Lr} and v_{Cr} in interval 2 are given by

$$i_{Lr3}(t) = \sqrt{\frac{C_r}{L_r + L_m}}\left(0.5V_{in} - v_{Cr2}(t_2)\right)\sin\omega_c(t-t_2) + i_{Lr2}(t_2)\cos\omega_c(t-t_2) \quad (13)$$

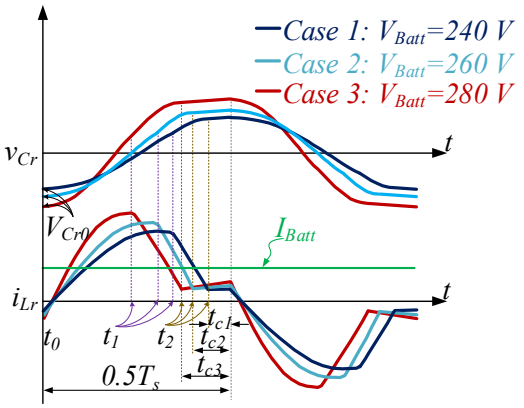

Fig. 6. The resonant current waveform in different cases with different circulating time.

$$v_{Cr3}(t) = 0.5 \cdot V_{in} - (0.5 \cdot V_{in} - v_{Cr2}(t_2)).\cos \omega_c (t - t_2) + \sqrt{\frac{L_r + L_m}{C_r}}.i_{Lr}(t_2).\sin \omega_c (t - t_2) \quad (42)$$

where $\omega_c = 1/\sqrt{(L_r+L_m)C_r}$ is the resonant angular frequency when L_m is in the resonance.

This interval is also called the circulating interval and it causes the increasing of conduction loss, so it should be considered to remove when designing the DBLLC converter.

By substituting the value of V_{Batt} into equation (3), (7), (11), the waveform of resonant current can be obtained in Fig. 6, with different values of the battery voltage meaning different values of circulating time in three cases. Case 3 is obtained when V_{Batt}=280V which has a longest circultaing time t_{c3}, case 2 is drawn at V_{Batt}=260V has circulating time t_{c2}, and case 1 at the point of V_{Batt}=240V has circulating time t_{c1} while t_{c2} longer than t_{c1}. The instant of t_2 is challenging to accurately define, this value depends on the impedance of L_r, L_m, resonant frequency, and the power. Because of the current control strategy, in the current constant mode (CC mode), the charging current I_{Batt} is controlled as a constant. Since the Ibatt is the average value of iSec which is the rectifier current of the resosnant current i_{Lr}, the larger peak value of i_{Lr} will result in the larger circulating period, and thus larger I_{Lr_rms}, as illustrated in Fig. 6. This is the reason why the existing of circulating period will cause an increasing of conduction loss.

III. Proposed Adaptive Frequency to Eliminate the Circulating Period

As aforementioned, the circulating period exists two times in one circle. Since in this period, there is no power transfer to the sencondary side of the DBLLC converter. Therefore, with the purpose of tranfering the same average battery current value means the longer circulating period results in a higher rms current flowing through the circuit. This means that all components and winding of transformer may suffer more conduction loss, thereby decreasing the efficiency of the whole converter. In this section, an adaptive frequency fa will be applied to remove this time interval of circulating.

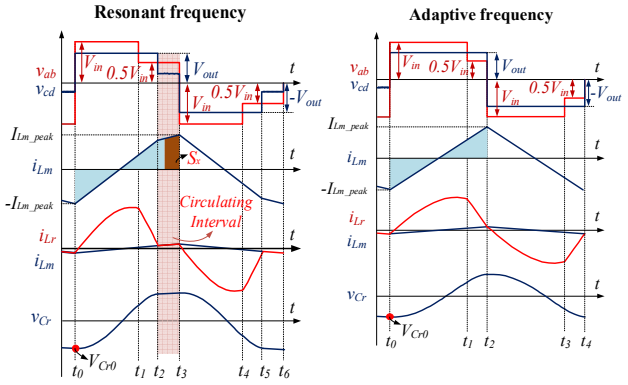

(a) (b)

Fig. 7. Waveforms of the components of the resonant tank when DBLLC converter operating at (a): resonant frequency and (b): adaptive frequency

A. Analysis the effects of circulating period and proposed adaptive frequency.

The existence of circulating period on each switching circle has major effects on the waveform of resonant component. With the idea of increasing the switching frequency so that switches will be forced to turn off at the time that the resonant current i_{Lr} become equal to the magnetizing current i_{Lm}, which means that the switching frequency will be raised larger enough to remove the interval 3, which is discussed in previous section.

Fig. 7 illustrates the different waveform of magnetizing current i_{Lm}, resonant current i_{Lr} and resonant voltage v_{Cr}. While Fig. 7a, the switching frequency equals resonant frequency, which has the circulating period, Fig. 7b is drawn when adaptive frequency is applied, thereby removing the circulating period. The different in the initial condition of the current and voltage of the resonant tank is the only parameter which lead to the different in the characteristic of i_{Lr} and also the v_{Cr}. There are two initial condition which must be defined to obtain the accuracy equation of i_{Lr} and v_{Cr}. It is the initial resonant capacitor voltage V_{Cr0}, and the initial resonant current $i_{Lr}(0)$, at $t=t_0$.

The $i_{Lr}(0)$ value when the adaptive frequency is applied could be easily define as

$$i_{Lr}(0) = I_{Lm\_peak\_fs=fa} = \frac{n \cdot V_o}{4 f_a L_m} \quad (13)$$

As shown in Figs. 7(a) and 7(b), the magnitude of $i_{Lr}(0)$ when $f_s=f_r$ and when $f_s=f_a$ is not much different. So it can be concluded that the $i_{Lr}(0)$ value is not the factor which significantly affect the difference when employing the adaptive frequency. The V_{Cr0} can be obtained by analyzing the charge variation Q_c of the resonant capacitor over half switching cycle. The waveform of capacitor voltage v_{Cr} has a half-wave symmetric characteristic:

$$v_{Cr}(t) = -v_{Cr}\left(t + T_s/2\right) \quad (14)$$

Thus, the Q_c can be obtained as

$$
\begin{aligned}
Q_c &= \left[v_{Cr}\left(T_s/2\right) - v_{Cr}(0) \right].C_r = -2V_{Cr0}.C_r \\
&= \int_0^{T_s/2} i_{Lr}(t)\,\mathrm{d}t = \int_0^{T_s/2} \frac{i_s(t)}{n}\,\mathrm{d}t + \int_0^{T_s/2} i_{Lm}(t)\,\mathrm{d}t \\
&= \frac{T_s}{2n.V_0}.\left(\frac{2}{T_s}\int_0^{T_s/2} V_0.i_s(t)\,\mathrm{d}t \right) + \int_0^{T_s/2} i_{Lm}(t)\,\mathrm{d}t \\
&= \frac{P}{2n.f_s.V_0} + \int_0^{T_s/2} i_{Lm}(t)\,\mathrm{d}t
\end{aligned}
\tag{15}
$$

Then we achieved the equation to define the initial condition of resonant voltage at conventional case V_{Cr0_c} when f_s=f_r as:

$$
V_{Cr0\_c} = -\frac{P}{4n.f_r.V_o.C_r} - \frac{\int_0^{T_s/2} i_{Lm}(t)\,\mathrm{d}t}{2C_r} = -\frac{P}{4n.f_r.V_o.C_r} - \frac{S_x}{2C_r} \tag{16}
$$

Where S_x is the area pointed out in Fig. 7. S_x exists due to the circulating interval. The longer CI means the larger S_x. The larger S_x means the resonant current and voltage is larger. When the converter is operated at adaptive switching frequency, the CI will be removed as shown in Fig. 7b. In this case, we have

$$
\int_0^{Ts/2} i_{Lm}(t)dt = 0 \tag{17}
$$

Therefore, the initial condition of the resonant voltage at proposed case V_{Cr0_p} when f_s=f_a can be obtained:

$$
V_{Cr0\_p} = -\frac{P}{4n \cdot f_a \cdot V_o \cdot C_r} \tag{18}
$$

From (16) and (18), the amplitude of V_{Cr0_p} is smaller than V_{Cr0_c}, which leads to the smaller of *rms* value of resonant current and resonant voltage. It means that the power loss in all devices will be reduced.

B. Gain characteristic and lookup table controlled of adaptive frequency.

Thanks to the PWM control strategy, the voltage gain of DBLLC resonant converter can be regulated in a wide range of switching frequency. At fixed switching frequency equal to resonant frequency, with the range of duty from 0 to 0.5, the converter can be able to regulate the range of voltage gain from 0.5 to 1. To regulating the same gain value, an increasing switching frequency f_s means an increasing duty is required. However, the duty value is limited in the range from 0 to 0.5, therefore, with too high value of fs will lead to the failing of systems, due to the duty can not regulate the proper gain. As a result, when f_s is increased, the maximum voltage gain will be limited. Another trade-off that needs to carefully consider is that the loss conflict. As mentioned before, with adaptive frequency, the rms current flowing through the circuit will be decreased, thus the conduction loss off all devices and winding loss will be decreased too. However, the switching loss and the transformer core loss will be increased. After carefully considering these trade-offs, the look-up table of f_a is obtained by numerical method which illustrated in Fig. 8, the gain characteristic versus duty in both case f_s=f_r and f_s=f_a is also drawn on this figure. When f_s is increased to fa, the duty must be larger than when f_s=f_r to regulate the same voltage gain value.

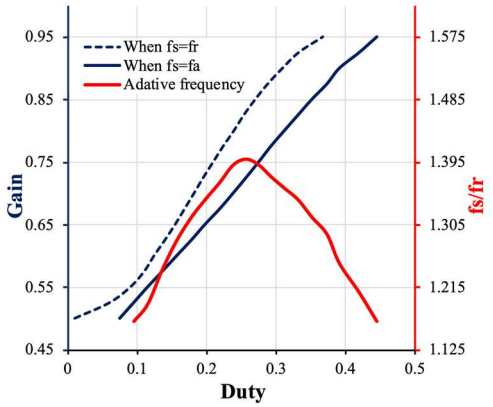

Fig.8. Gain characteristic varies with the different of switching frequency.

Based on the gain characteristic which is illustrated in Fig. 8, the frequency lookup table strategy can be adopted to control the operating frequency of the DBLLC converter, while the duty is still regulated by control the charging current of battery.

IV. Simulation and Experimental Results

A. Simulation Results

Simulation is performed by Psim 9.0 to verify the proposed control method. The parameters for simulation are presented in Table 1.

TABLE I
RATING AND PARAMETERS OF DBLLC CONVERTER

Parameters	Value
V_{Link}	*400 VDC*
V_{Batt}	*360 VDC*
L_r	*4.5 uH*
L_m	*140 uH*
C_r	*0.6 uF*
f_s	*100 kHz*
f_a	*100 kHz*
Power-rating	*7.4 kW*

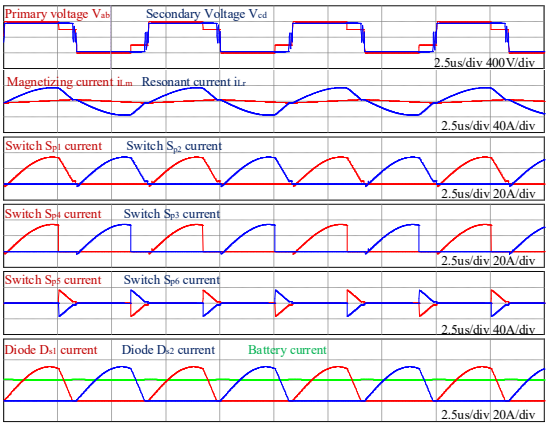

(b)

Fig. 9. Gain characteristic varies with the different of switching frequency.

Simulation is performed by Psim 9.0 software to verify the proposed control method. The parameters for

simulation are presented in Table 1. Fig. 9 shows the primary voltage V_{ab} and secondary voltage V_{cd}, the resonant current i_{Lr}, the magnetizing current i_m and the power switches current. In this simulation, the switching frequency is selected equal to resonant frequency. Hence, the circulating current is eliminated.

B. Experimental results

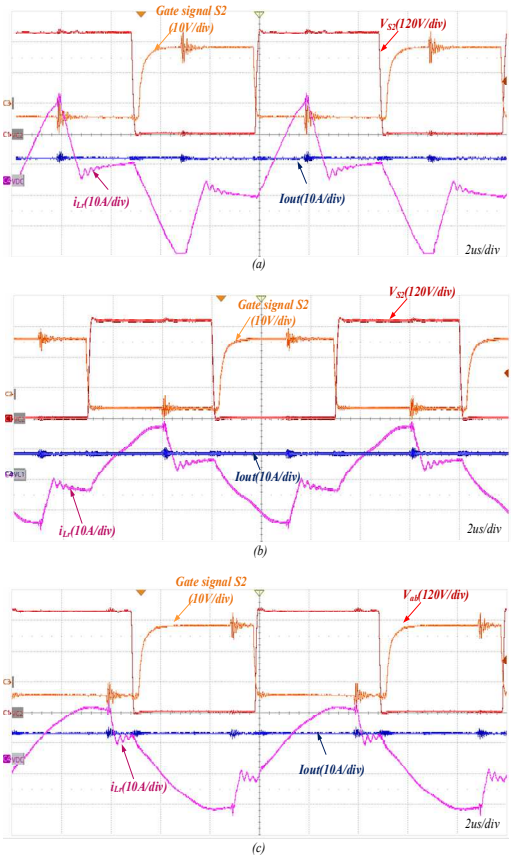

Fig. 10. Experimental results with different power (a) 2 kW (b) 2.6 kW (c) 3.3 kW.

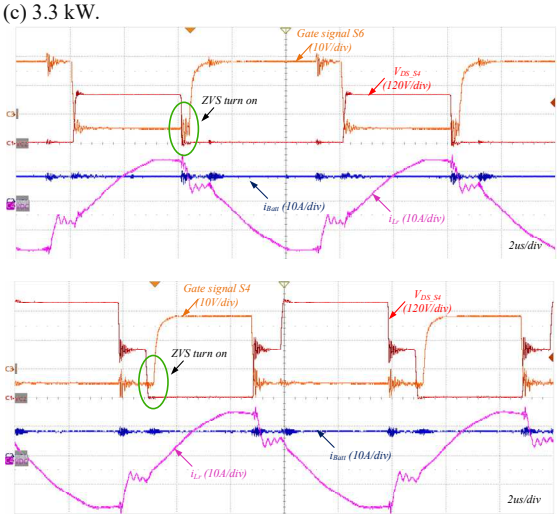

Fig. 11. Experimental results of gating signals with output power 3.3 kW.

The experimental prototype was built to examine the operating principle and the performance of the converter. The DBLLC converter is controlled by programing in the DSP of TMS32028377D of Texas instrument. Due to the limitation of the hardware setup, the power rating in experimental setup is 3.3 kW. The DBLLC converter is experimented at different load to demonstrate the analysis that the value of circulating time is varied at different battery voltage. Figs. 10(a), 10(b) and 10(c) show the waveform of resonant current, load current and gate signals at output power of 2 kW, 2.6 kW and 3.3 kW, respectively. It can be seen that the circulating time decrease when the power-rating increase. These experimental results demonstrated that the longer circulating time means the higher i_{Lr_peak} then also the higher $i_{Lr\_rms.}$. The experimental results of gate signals and the drain source voltage of switch S_2, S_4 are shown in Fig. 11. As shown in this figure, all switches achieved ZVS turn on.

V. Conclusions

In this paper, the DBLLC converter operating at adaptive frequency is demonstrated to be a good converter to apply in an OBC system because of its advantages such as: high quality, high density, and low losses, ... The detailed analysis of the impact of circulating period is also presented in this paper. The simulation and the experimental results demonstrated the performance of the DBLLC and the proper of applying the adaptive frequency when operating the DBLLC converter, all semiconductor switches achieve the ZVS turn-on.

Acknowledgment

We acknowledge the support of time and facilities from Ho Chi Minh City University of Technology (HCMUT), VNU-HCM for this study.

References

[1] "The electric vehicle world sales database, EV volumes.com", 2021, EV-Volumes - The Electric Vehicle World Sales Database.

[2] Alireza Khaligh and Michael D'Antonio, "Global Trends in High-Power On-Board Chargers for Electric Vehicles", IEEE Transactions on Vehicular Technology, vol. 68, no.4, April 2019.

[3] Jun-Sung Kim, Chang-Yeol Oh, Won-Yong Sung, Byoung Kuk Lee, "Topology and Control Scheme of OBC-LDC Integrated Power Unit for Electric Vehicles", IEEE Trans Power Electronics, April 3, 2016.

[4] D. Gu, Z. Zhang, Y. Wu, D. Wang, H. Gui and L. Wang, "High efficiency LLC DCX Battery Chargers with Sinusoidal Power Decoupling Control", 2016 IEEE Energy Conversion Congress and Exposition (ECCE), Milwaukee, WI, 2016, pp. 1-7.

[5] Junjun Desng, Siqi Li, Sideng Hu, Chunting Chris Mi and Ruiquing Ma, "Design Methodology of LLC Resonant Converters for Electric Vehicle Battery Chargers", IEEE Transactions on Vehicular Technology, vol.63, no.4, May. 2014.

[6] Fariborz Musavi, Marian Craciun, Deepak S. Gautam, Wilson Eberle, and William G. Dunford, "An LLC resonant DC-DC Converter for Wide Output Voltage Range Battery Charging Applications", IEEE Transactions on Power Electronics, vol. 28, no. 12, December 2013.

[7] Yuqui Wei, Quanming Luo, and Alan Mantooth: "Overview of Modulation Strategies for LLC Resonant Converter" IEEE Transactions on Power Electronics, vol. 35, no. 10, October 2020.